



OPEN ACCESS

EDITED BY

Yunhui Zhang,
Southwest Jiaotong University, China

REVIEWED BY

Cong Zhang,
Hohai University, China
Sun Wenjibin,
Guizhou University, China
Cheng Zeng,
The University of Newcastle, Australia
Shiyuan Huang,
Chongqing Jiaotong University, China

*CORRESPONDENCE

Meng Zhao,
zhaomeng@cdu.edu.cn

SPECIALTY SECTION

This article was submitted to
Geohazards and Georisks,
a section of the journal
Frontiers in Earth Science

RECEIVED 13 May 2022

ACCEPTED 22 July 2022

PUBLISHED 13 September 2022

CITATION

Zhao M, Wu H-G, Guo W, Tan B-R, Hu C,
Deng R and Chen L-Y (2022),
Experimental study of the particle
agglomeration on its mechanical
properties of collapsible loess.
Front. Earth Sci. 10:943383.
doi: 10.3389/feart.2022.943383

COPYRIGHT

© 2022 Zhao, Wu, Guo, Tan, Hu, Deng
and Chen. This is an open-access article
distributed under the terms of the
[Creative Commons Attribution License
\(CC BY\)](https://creativecommons.org/licenses/by/4.0/). The use, distribution or
reproduction in other forums is
permitted, provided the original
author(s) and the copyright owner(s) are
credited and that the original
publication in this journal is cited, in
accordance with accepted academic
practice. No use, distribution or
reproduction is permitted which does
not comply with these terms.

Experimental study of the particle agglomeration on its mechanical properties of collapsible loess

Meng Zhao ^{1,2*}, Hong-Gang Wu ³, Wei Guo ²,
Bo-Ren Tan ¹, Cheng Hu ¹, Rui Deng ¹ and
Li-Yi Chen ²

¹Sichuan Engineering Research Center for Mechanical Properties and Engineering Technology of Unsaturated Soils, Chengdu University, Chengdu, China, ²State Key Laboratory of Geo-Hazard Prevention and Geo-Protection, Chengdu University of Technology, Chengdu, China, ³China Northwest Research Institute Co., Ltd of CREC, Lanzhou, China

Loess, distributed all over the world, exhibits the behavior that is related to their formation history, mineralogy, and microstructure, which can cause serious geotechnical engineering problems. This paper presents the Baozhong railway is a key transportation channel for Guyuan city in Ningxia province of northwestern China. Based on field investigations treasure middle section of the railway in the study area, it is found that the more serious diseases subgrade settlement, local roads embankment platform dislocation occurs and lots of cracks were founded. For several years, with the train speed increasing, and due to the influence of widespread flood irrigation on the farmland, the subgrade experienced a degree of settlement. This settlement was not alleviated after three treatments, which seriously affected train safety. In order to analyze the reason for the railway line settlement, soil samples were collected from the collapsible loess subgrade. Consolidation test, particle size analysis test, X-ray diffraction test (XRD), and scanning electron microscopy test (SEM) were performed to investigate the mechanism of the subgrade disease. The results reveal that loess collected from severe differential settlements at locations has a highly compressible, and its clay content and agglomeration level was generally low. These results illustrated that the particle size of 20–50 microns has a direct effect on its mechanical properties of loess. This part of the particles has a cementation effect. It can effectively connect the large particles of the skeleton to form particle agglomerates and is an effective composition of loess clay minerals. Therefore, the loess structure was not stable due to its relatively low internal molecular attraction. When such saturated collapsible loess subgrade subjected to train vibration load, the soil might be liquefied, and its structure might be instable. If the drainage of the subgrade was not well designed, severe differential settlements would occur. The research is of great significance to clarify the relationship between loess particle composition, microstructure and its macromechanics, providing a vital reference for the engineering construction in the loess-dominated areas.

KEYWORDS

particle agglomeration, mechanical properties, existing railway line, collapsible loess, experimental study

1 Introduction

Loess is found all over the world, this soil exhibits behavior that is related to their formation history, mineralogy, and microstructure, which can cause serious geotechnical engineering problems (Zhao et al., 2020). In the loess area, many engineering diseases occurred due to its collapsibility behavior, such as widespread distribution of the ground cracks, deformation of urban buildings, landslides caused by rain or irrigation, subgrade settlement of highways and railways (Derbyshire, 2001; Delage et al., 2005; Sun et al., 2009). With the development of cities around the world, the demand for municipal, highway, railway is also growing. The construction will have more problems associated with the collapsible behavior of the loess in this area.

Water shortage is common around world, especially in the northwest China (He et al., 2020; Zhang et al., 2021a, 2021b; Yao et al., 2022). A balance between a reasonable flow rate for irrigation and the effective loess collapse control is a challenge in this area. Loess collapse is a concern in China and other countries. Guyuan, an important city of the Belt and Road trade route, is a key city for rail transport, where loess is widely distributed. With the development of transportation such as the Baozhong railway, many subgrade diseases spread in the last 2 decades. The K329-K331 section of the Bao Zhong railway is situated in the Malian town of Guyuan City (Figure 1). Due to weather changes and irrigating activities, the ground water level in this area and the moisture content of the railway loess subgrade are not stable. Differential or uneven settlements may occur along the railway, when the saturated collapsible loess subgrade is subjected to dynamic loads induced by trains. Placing additional railway slag to re-level the low portions induced by the differential settlements was a routine maintenance work in this area. After many years of the maintenance activities, additional static railway slag loads became significant, and the potential of differential settlements might be more severe in this area (Zhao et al., 2019). In addition, the railway loads were increased significantly in last few decades. As a result, the differential settlement in this area has become a severe threat on the safety operation of the railway. Therefore, In order to treat the differential settlements in this area, the study on the collapsibility mechanism of loess under train load conditions and the uneven settlement of Baozhong Railway are extremely urgent for the development of railway transportation in Ningxia, China.

Many researches were completed on loess in China and other countries (Wen and Yan, 2014). Hu (2005), Lommler and Bandini (2015), Li et al. (2016) studied the mechanism of loess collapse and researches mainly focused on the particle composition, pore characterization, and porosity of loess. Silt with particle sizes between 0.05 and 0.01 mm was considered critical on the

behavior of loess (Zhao and Lei, 2011; Jiang M. et al., 2014). The composition of loess determined its mechanical and chemical properties, especially quartz and feldspar, which consisted of the skeleton composition of soil (Zhang et al., 2018). Clay minerals are mainly, illite, chlorite, rock, water mica, etc. They wrapped in particulate matters around the soil to determine the water sensitivity (Sun, 2010; Muñoz-Castelblanco et al., 2012). The mineral compositions of loess encountered in different areas of China were almost the same. However, the content of the microcrystalline calcium carbonate showed an increasing trend from the southeast to the northwest. Using polarized light, microscopic and scanning electron microscopy, Susan (2017) found that the coarse calcium carbonate was important as a support skeleton, and the native microcrystalline calcium carbonate played a role in cementing soil particles. The size, shape, distribution and structure of pores directly affected the permeability, collapsibility and other related geotechnical engineering properties of loess Romero and Simms (2008). The mechanical properties of loess were closely related to their microstructure. Luo et al. (2018) and Assadi-Langroudi et al. (2018) mainly explored the microstructure of the loess with a polarizing microscope. Romero and Simms (2008) and Xie et al. (2018) had a more detailed view on description and classification of the microstructure of loess. They found that the microstructure characteristics of loess were directly related to the loess collapsibility, and the arrangement of soil particles also played an important role. Jiang MJ. et al. (2014) observed the loess in Xi'an area by polarizing mirror and scanning electron microscope, he founded that the coarse particles of Q₂ loess in Xi'an area was mainly less attached and dispersed. Ye et al. (2012), Zhuang et al. (2018) quantitatively studied the microstructure parameters and macroscopic characteristics of loess. They found that the macro-mechanical properties and the microstructure of loess were closely related. The research on collapsible loess in China and other countries were mainly focused on the experiments and analyses of the loess. Limited studies have been conducted to understand the mechanism of the loess collapses.

In this paper, from a mesoscopic-microscopic perspective, macroscopic and microscopic test methods are used to analyze the occurrence mechanism of subgrade disease in collapsible loess in serious diseased areas. The results of this study are of great significance for the prevention and control of loess subgrade collapse.

2 Engineering geological background

The study area was the K329~K331 section of Bao Zhong railway which is located at the Malian town of Guyuan city

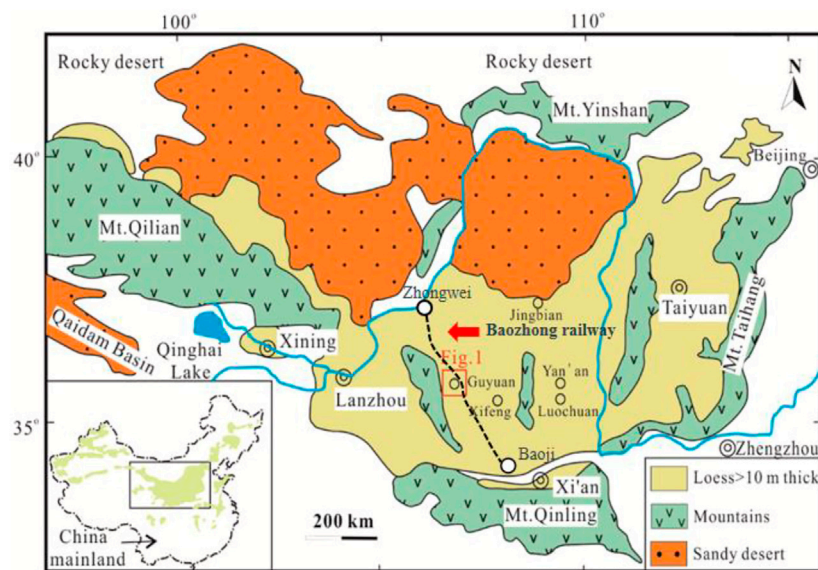


FIGURE 1
Shows Google earth map of the study area (Zhao et al., 2020).

(Figure 1), east of the Qingshui River. The starting point in the southeast was Baoji in Shaanxi Province, after passing through Pingliang City, Gansu Province, and the furthest end of the northwestern side was the town of Luobao in Zhongwei County, Ningxia Province (Zhao et al., 2020).

The location is at the Xiji Basin on the northwestern edge of the Loess Plateau in China, northeastern margin of Tibet Plateau (Yan et al., 2017; Zhang et al., 2022). The climate in the study area is characterized by a semi-arid and semi-humid continental climates with predominantly summer rainfall. About seventy percent of rainfall occurs within June to September. Due to water scarcity, large-scale farmland irrigation is required every spring and autumn for agricultural crops, which causes the rising of the groundwater level. A proliferation of loess disease had occurred along the railway line (Figure 2). Due to the influence of widespread flood irrigation on the farmland, the subgrade had a degree of settlement. The settlement had not been alleviated after three treatments. The “three treatment methods” are actually high-pressure jet grouting. High-pressure jet grouting is a method of treating ground with a high-pressure cement slurry sprayed from a horizontal nozzle through a drill pipe to form a jet stream, cutting the soil and mixing it with the soil. The lime soil water retaining wall for the foot of subgrade and grouting reinforcement for the hard shoulder were used at the three treatments. The lime soil water retaining wall for the foot of subgrade and grouting reinforcement for the hard shoulder were used at the three treatments (Zhao et al., 2020). Additionally, after many years of subgrade

subsidence, the railway subgrade had produced uneven settlement, which leads to uneven tracks (Figure 2A), and worse: there were many cracks on both sides of the roadbed (Figures 2B,C). The longest extension of the crack was about 600 m long. The warning signs on both sides of the railway sink down with the maximum sinking level being 1.5 m. In addition, traffic safety is seriously threatened. For these reasons, the cause of the uneven settlement for the Baozhong railway subgrade loess is in urgent need of being addressed.

3 Sample preparation and methods

Three samples (Sample numbers 1, 2, and 3) were selected at Station K331 + 530, where significant roadbed diseases were observed (called the disease segment in this paper) (shown in Figure 3). For comparison, another three samples (Sample numbers 4, 5, and 6) were selected at Station K331 + 585, where no or limited roadbed diseases were observed (called the non-disease segment in this paper) (shown in Figure 3). These six samples were obtained at depths of 3 m, 6 and 9 m. The information of these six samples was shown in Table 1 below.

3.1 Test methods

Consolidation test, particle size analysis test, XRD diffraction test and SEM scanning electron microscopy test



FIGURE 2
Subgrade disease of Baozhong railway. (A) uneven track; (B,C) cracks on both sides of the subgrade.



FIGURE 3
Sampling on site.

were performed in this study. Detailed descriptions for these tests are as follows:

3.1.1 Consolidation tests

WG (WG-1C) single lever consolidation instrument was used in this study. The sample was prepared by a $\phi 61.8 \text{ mm} \times 20 \text{ mm}$ ring knife. The applied consolidation pressures were 50, 100 and 200 kpa.

3.1.2 Particle size analysis tests

The Mastersizer 2000 Laser Grain Size Analyzer was used in the grain size distribution tests. Firstly, the specimen was dried in a drying oven, pulverized, and passed through a 1 mm sieve. Secondly, a 15 g powder specimen was taken into the test chamber of the laser grain size analyzer. Finally, the percentage of the total volume of the soil grains of each grain size was ascertained by laser diffraction.

TABLE 1 The basic situation of the sample.

Sample number	Mileage number	Subgrade type	Sampling depth	Disease degree
1	K329 + 530	Disease segment	3	slight
2	K329 + 530	Disease segment	6	serious
3	K329 + 530	Disease segment	9	serious
4	K331 + 585	Non-disease segment	3	no
5	K331 + 585	Non-disease segment	6	slight
6	K331 + 585	Non-disease segment	9	slight

TABLE 2 Consolidation test parameters.

Sample number	Coefficient of consolidation	Coefficient of compressibility	Compression modulus
1	4.02	0.383	3.702
2	1.95	0.500	2.951
3	3.27	0.445	3.322
4	3.78	0.299	4.918
5	3.66	0.430	3.411
6	3.47	0.402	3.522

3.1.3 XRD diffraction tests

This test was conducted using a stoichiometric DMAX-3C diffractometer, in which CuK α and Ni were used to diffract at a diffraction angle range, between 5° and 60°. The obtained data was analyzed by a MID Jade software.

3.1.4 Scanning electron microscopy tests

The test samples were placed on Hitachi S-3000 N scanning electron microscope, and the photomicrographs were observed in a high vacuum mode. Photographs were taken with different magnification for each representative area of each sample.

4 Test results and discussion

4.1 Compressibility

The compressibility of the soil is generally determined by the compressive modulus, E_s : $E_s \leq 4$ MPa is a highly compressible soil; $20 \text{ MPa} \geq E_s \geq 4$ MPa is moderate compressible soil; and $E_s \geq 20$ MPa is lowly compressible soil. Consolidation test results were shown in Table 2.

The results revealed that samples 1, 2, and 3 in the disease segment, and Samples 5 and six in the non-disease segment were highly compressible soils. The compressive modulus of samples 2 and 3 was lower than that in samples 1, 5, and 6, indicating a relative high compressibility of these

two samples. It is understood that the compressibility of a soil was directly related to its internal pores. The higher the compressibility, the larger the void ratio of a soil. It could be concluded that samples obtained in the disease segment were generally highly compressible with a relatively high void ratio. Therefore, relatively severe differential settlements were observed.

Relatively high compression index was achieved from Samples 5 and 6, which were obtained at the non-disease segment. However, the shallowest sample (Sample 4 at a depth of 3 m) at this non-disease segment did not show a high compression index. Therefore, it can be concluded that soils at a relatively shallow depth played a critical role on the subgrade performance. A better railway performance could be expected, where a stiff soil layer existed near the ground surface, even a relatively highly compressible soil lied underneath it. It is understood that the performance of the roadbed might be affected by the flood, irrigation activity and the dynamic loads induced by trains. The differential settlements might be related to the soil particles composition. The particle structure might be related to the porosity of soil.

4.2 Grain distribution

The grain size gradation curve and the particle distribution curve of the six test samples were plotted and shown in Figure 4.

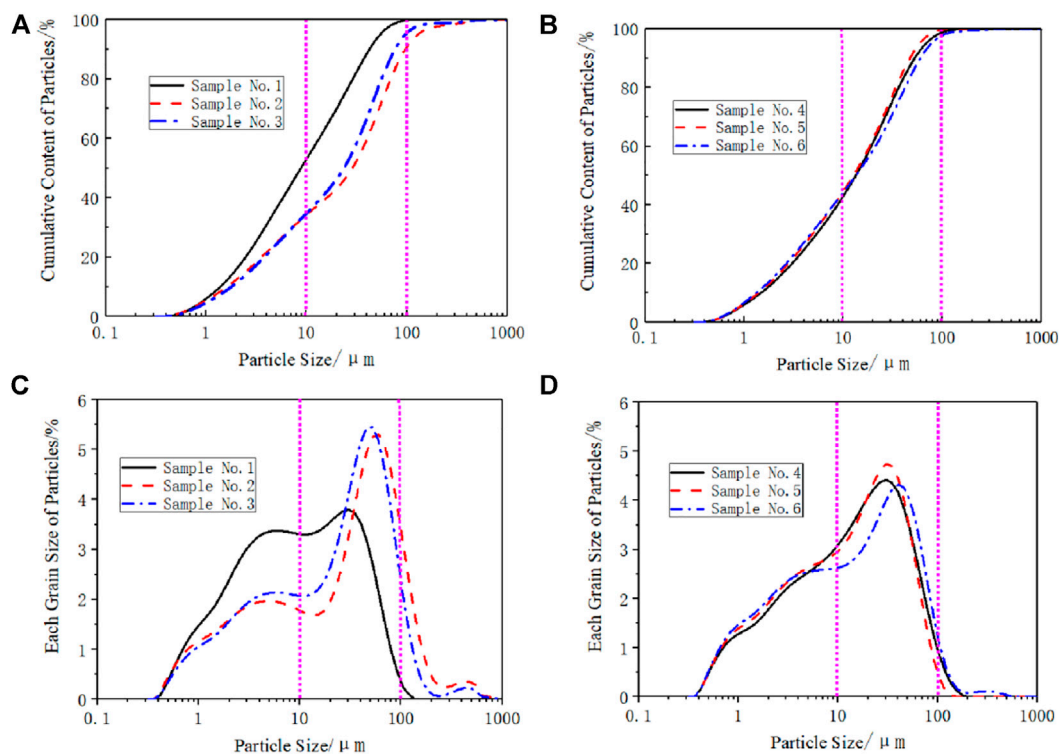


FIGURE 4 (A) Logarithmic curve of the particle size distribution on samples at disease segments, (B) Logarithmic curve of the particle size distribution on samples at non-disease segments, (C) Cumulative logarithmic curve of the particle size distribution on samples at disease segments, and (D) Cumulative logarithmic curve of the particle size distribution on samples at non-disease segments.

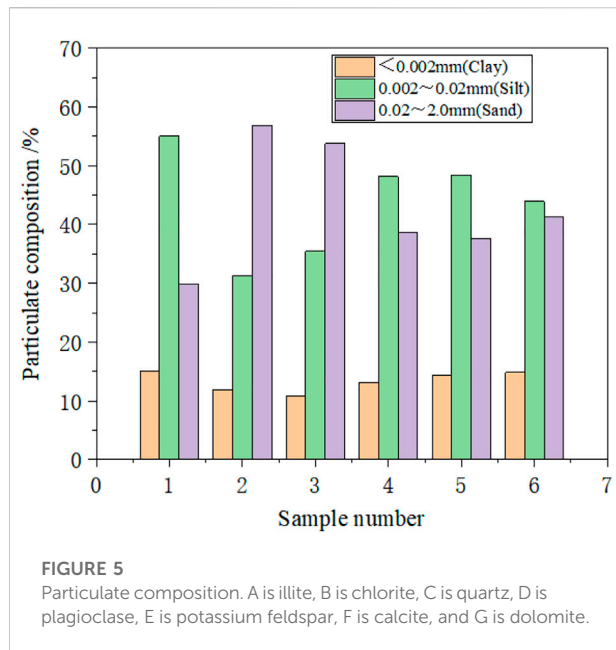
TABLE 3 Particle size analysis parameters.

Sample number	Nonuniformity coefficient	Curvature coefficient	Clay content (%)	Silt content (%)	Sand content (%)
			< 0.002 mm	0.002 ~ 0.02 mm	0.02 ~ 2.0 mm
1	9.12	0.76	15.04	55.03	29.91
2	23.98	0.87	11.89	31.20	56.90
3	19.42	0.93	10.75	35.49	53.74
4	12.02	1.00	13.07	48.17	38.74
5	12.91	0.93	14.40	48.36	37.59
6	15.84	0.75	14.80	43.90	41.29

The particle size analysis data are summarized in Table 3 and Figure 4.

As shown in Figures 4A,B, the particle size distribution curves of Samples 2 and 3 in the disease segment appeared to be less smooth than those of Samples in the non-disease segment. As shown in Figures 4C,D compared to samples in the non-disease segment, the

content of the small size particles (<50 μm) of Samples 2 and 3 in the disease segment were relatively low, but the big size particles (>100 μm) of them were relatively high. Therefore, it was considered that due to the low clay contents, the internal molecular attraction in Samples 2 and 3 might be relatively small, resulting in a relatively poor performance of a railway subgrade.



According to [Table 3](#) and [Figure 5](#), the results reveal that Samples 2 and 3 had relatively low clay contents and relatively high sand contents compared to other samples. From the soil structure perspective, the loess has a relatively high sensitivity to water. In samples 2 and 3, the clay content might be not enough to fill the voids between sand and silt, and the internal molecular attraction was small. This may be part of the reason that samples 2 and 3 showed high compressibility, and severe subgrade diseases were observed in this segment of the railway.

4.3 Mineral composition

XRD diffraction tests were carried out on all samples, and the results were shown in [Figure 6](#). The results indicated that the samples in the diseased area were quite different from those in the non-disease area. Significant differences can be observed on Samples 3 and 3 compared to other samples.

[Figure 6](#) showed that the maximum values was basically the same for all samples. The maximum values of Samples 2 and 3 in the disease segment were relatively higher than others, the maximum values of Samples 1, 5, and 6 were similar, and the maximum value of Sample 4 was the lowest.

The maximum diffraction value ($A + B + C$) was the sum of illite, chlorite and quartz, respectively. This value reflected the degree of crystallization of the sample. Since the degree of crystallization of quartz was greater than that of illite and chlorite, a great maximum diffraction value indicated a relatively great quartz contain of a sample, based on results shown in [Figure 6](#), compared to other samples, Samples 2 and

3 in the disease segment contained more quartz, but less calcite. The content of plagioclase, potassium feldspar, and dolomite in all samples were almost the same. This result indicated that the contents of illite, chlorite, quartz, and calcite might affect the subgrade performance.

[Table 4](#) showed that Samples 2 and 3 contained more than 50% of quartz and only approximately 25% of cohesive particles, which were generally formed of chlorite and illite. This result was consistent with the results of particle analysis test, in which Samples 1, 2, and 3 in the disease segment contained relatively larger size particles compared to other samples. The quartz content of Samples in the non-disease segment was relatively low (<46%) but chlorite and illite based clay mineral contents were relatively high (between 35 and 42%). Therefore, it was considered that relatively high clay mineral content was likely to increase the destructive resistance of a soil and improve the performance of the railway subgrade.

4.4 Microstructure

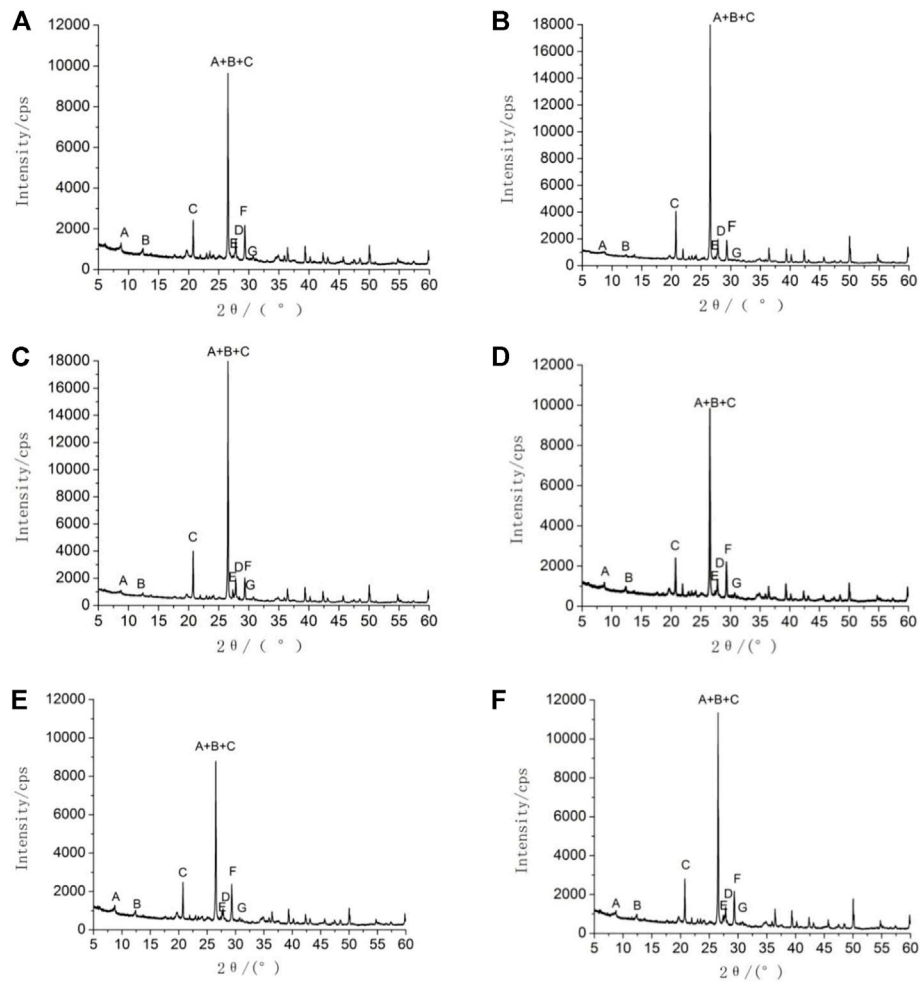
4.4.1 Micro qualitative analysis

In order to further study the mechanism of the disease loess subgrade soil, the scanning electron microscopy (SEM) was performed on Sample 2 in the disease segment. As a comparison, SEM was also performed on Sample 5 in the non-disease segment. [Figure 7](#) and [Figure 8](#) showed the details of the SEM results.

[Figure 7](#) showed that the microstructure of sample 2 in the diseased area was dominated by the structure type of scaffolds with large pores and micro-cementation or weakly cemented, with low connection strength. The contact surface is very small, and the particles support each other, sometimes in point contact, and sometimes in edge and edge contact, forming relatively large interparticle pores. At the same time, due to the relatively high sand content, there are few clay cements between the particles, and the cements fill the pores between the particles sporadically, showing micro-cementation; the skeleton particles are mainly composed of single granular particles under the microscope. It has the characteristics of sand-like, the shape is relatively clear, and the particle size is relatively uniform.

[Figure 8](#) showed that the microstructure of Sample 5 in the non-disease segment was strong and honeycomb. The skeleton particles in the microstructure are composed of agglomerates formed by the agglomeration of small particles, and there are certain large pores and small pores. The agglomerated particles are connected by cementing substances, and the graininess is not obvious. At the same time, the content of clay particles in the cement is the highest, and the particles are aggregated. The skeleton particles are embedded in the cement and do not contact each other. The connection strength is the highest.

From the above, it can be clearly seen that the loess samples in the diseased area and the non-disease area have detailed



A is illite, B is chlorite, C is quartz, D is plagioclase, E is potassium feldspar, F is calcite, and G is dolomite.

FIGURE 6

XRD diffraction patterns from samples in the disease segment (a, b, c) non-disease segment (d, e, f):(A) sample No. 1,(B)sample No.2, (C) sample No.3, (D) sample No. 4, (E) sample No.5, (F) sample No.6.

TABLE 4 Percentage of material composition derived from XRD diffraction.

Sample number	Illite (%)	Chlorite (%)	Quartz (%)	Potash feldspar (%)	Plagioclase (%)	Dolomite (%)	Calcite (%)
1	29	13	38	1	7	1	11
2	22	4	57	1	8	1	8
3	19	6	54	2	8	2	9
4	21	11	44	1	7	2	14
5	29	11	40	1	5	1	13
6	21	12	46	3	7	1	12

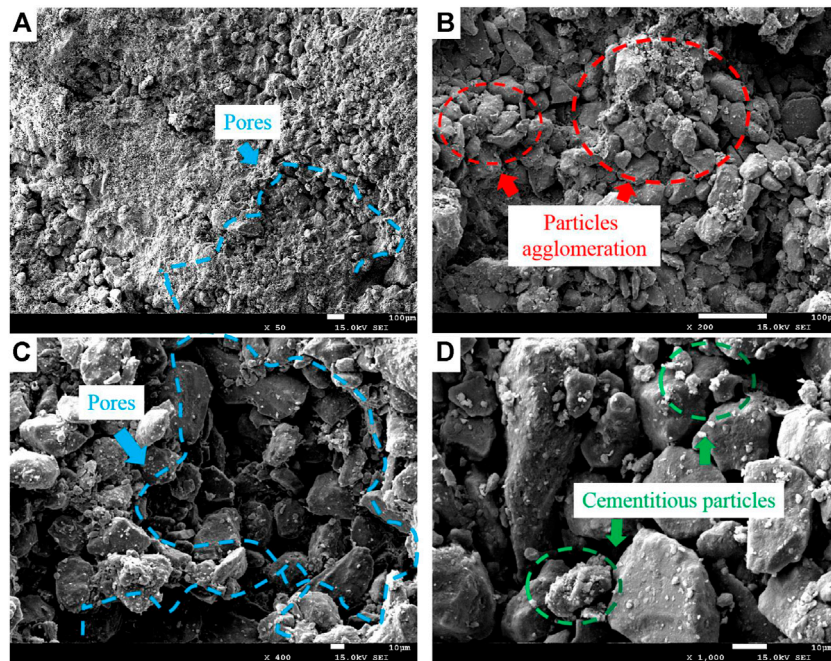


FIGURE 7
 Electron microscopic scanning of the sample at disease segment:(A) Sample No.2–50 times, (B) sample No.2–200 times, (C) sample No.2–400 times,(D) sample No.2–1,000 times.

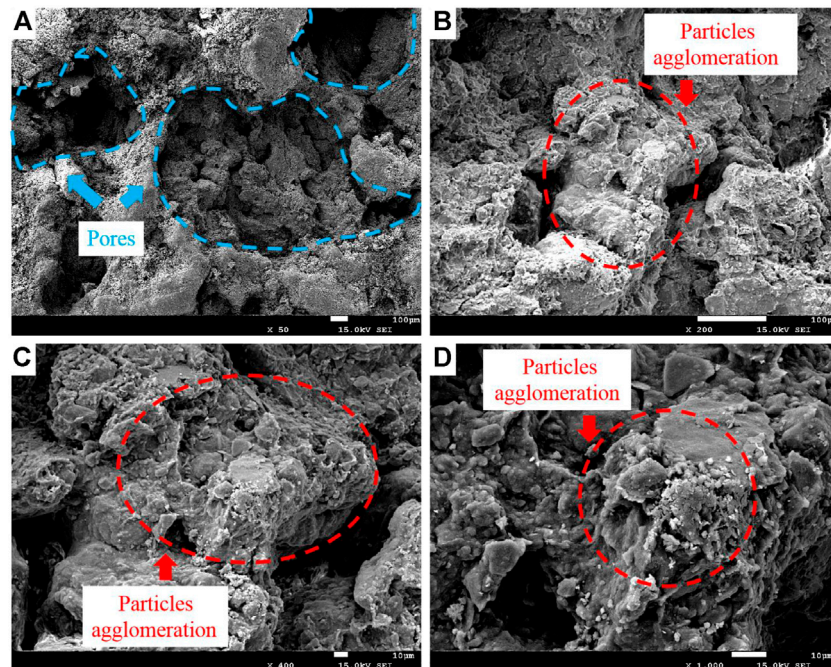


FIGURE 8
 Electron microscopic scanning of the sample at non-disease segment:(A) Sample No.5–50 times, (B) sample No.5–200 times, (C) sample No.5–400 times, (D) sample No.5–1,000 times.

TABLE 5 Micro characteristic parameters.

Sample number	Entropy	Area ratio		Roundness	
		Particles	Porosity	Particles	Porosity
2	1.95	0.59	0.41	1.34	1.42
5	1.41	0.8	0.2	1.3	1.39
Sample Number	Distribution fractal dimension		Degree of orientation		Euler number
	Particles	Porosity	Euler number	Porosity	
2	0.22	0.54	0.97	0.95	0.31
5	0.21	0.7	0.97	1.01	0.52

microstructure differences. The non-disease area is the loess roadbed with good mechanical properties, and its loess microstructure was more blurred compared to samples in the disease segment. Flake like particles were mainly covered by dust grains. The pore sizes were generally between 10 and 50 μm . They were mainly uniformly distributed, generally irregular or elongated, and well connected. As shown in Figures 8C,D, clay size particles filled the majority of the relatively big pores in the Sample 5, which was obtained from the non-disease segment. Therefore, the internal molecular attraction of this sample should be better than that in the disease segment.

4.4.2 Micro quantitative analysis

The obtained relevant microcosmic characteristic parameters from Sample 2 in the disease segment and sample 5 in the non-disease segment were summarized in Table 5.

As shown in Table 5, the porosity of Sample 2 in the disease segment was 0.41, which was obviously more than that of Sample 5 in the non-disease segment. The fractal dimension of grain and pore distribution of Sample 2 in the disease segment was larger than that in the non-disease segment, indicating that the soil particles in the disease segment were more dispersed, and the internal molecular attraction was relatively low. The porosity of the degree of orientation of Sample 2 in the disease segment was 0.54, which was significantly lower than that in the non-disease segment. The pores were small and in a disordered manner, and their connectivity was poor, indicating that the soil might have a poor drainage. The Euler numbers of Sample 2 in the disease segment was smaller than that in the non-disease segment, implying that the internal molecular attraction of Sample 2 in the disease segment was poor.

5 Discussions

5.1 Quantitative analysis of the agglomerated clay

The form of the particle connection has direct point-contact, direct surface contact, indirect point contact and

indirect surface contact (Shao et al., 2018). The direct contact refers to the interface between particles with limited cohesion. The indirect contact is the interface between particles having a film which consists of clay and salt crystal. The point and surface contacts stand for particle interfaces with relatively small and large contact areas, respectively. Those contact forms are shown in Figure 9.

Clay particles with direct or indirect contact surfaces may form a group of soil particles. This is called clay “agglomeration” in this paper. SEM scanning electron microscopy images showed a relatively low content of clay films and sheets of Sample 2 at the disease segment, and thus, the level of clay “agglomeration” of this sample was relatively weak. The voids between soil particles of Sample 5 in the non-disease segment were filled with clay films and sheets and the interfaces between soil particles were mainly surface contacts. Some soil particles in Sample 5 were completely wrapped with clay minerals. Therefore, the level of clay “agglomeration” of Sample 5 was strong. The clay “agglomeration” effects of the two Samples were shown in Figure 10.

As shown in Figures 10A,B, the soil clay mineral content and the clay “agglomeration” level of Sample 2 in the disease segment were relatively low, resulting in a weak cohesion. The structures of such saturated soil might be liquefied and unstable under dynamic loads. It could also be observed from Figures 10C,D that the clay “agglomeration” level of Sample 5 in the non-disease segment was relatively high. A strong connection between soil particles was formed, resulting in a strong cohesion between soil particles. A better performance was expected for such soil used as a railway subgrade.

5.2 Qualitative analysis of the agglomerated clay

The results of the particle size analysis tests and the XRD tests showed that the contents of clay minerals and quartz particles of the samples in disease segment and those in the non-disease segments were not the same, resulting in their different

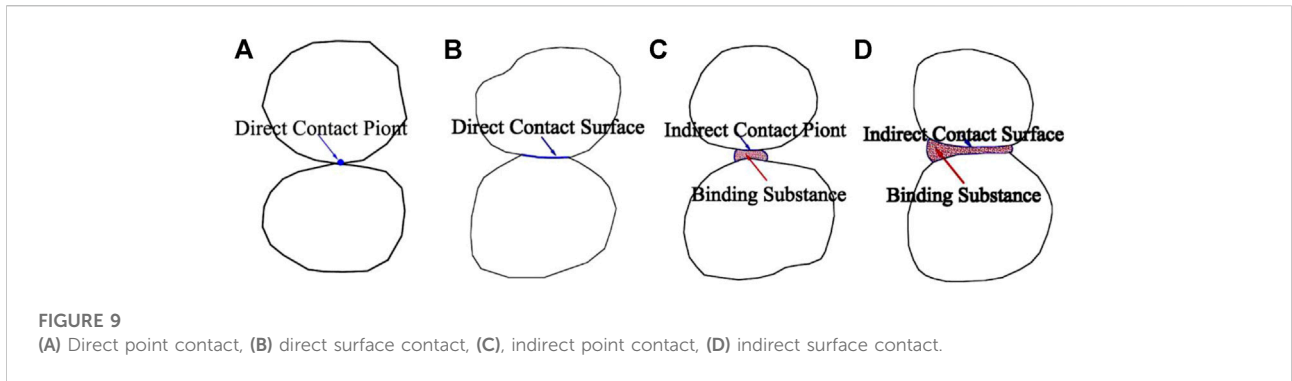


FIGURE 9
 (A) Direct point contact, (B) direct surface contact, (C), indirect point contact, (D) indirect surface contact.

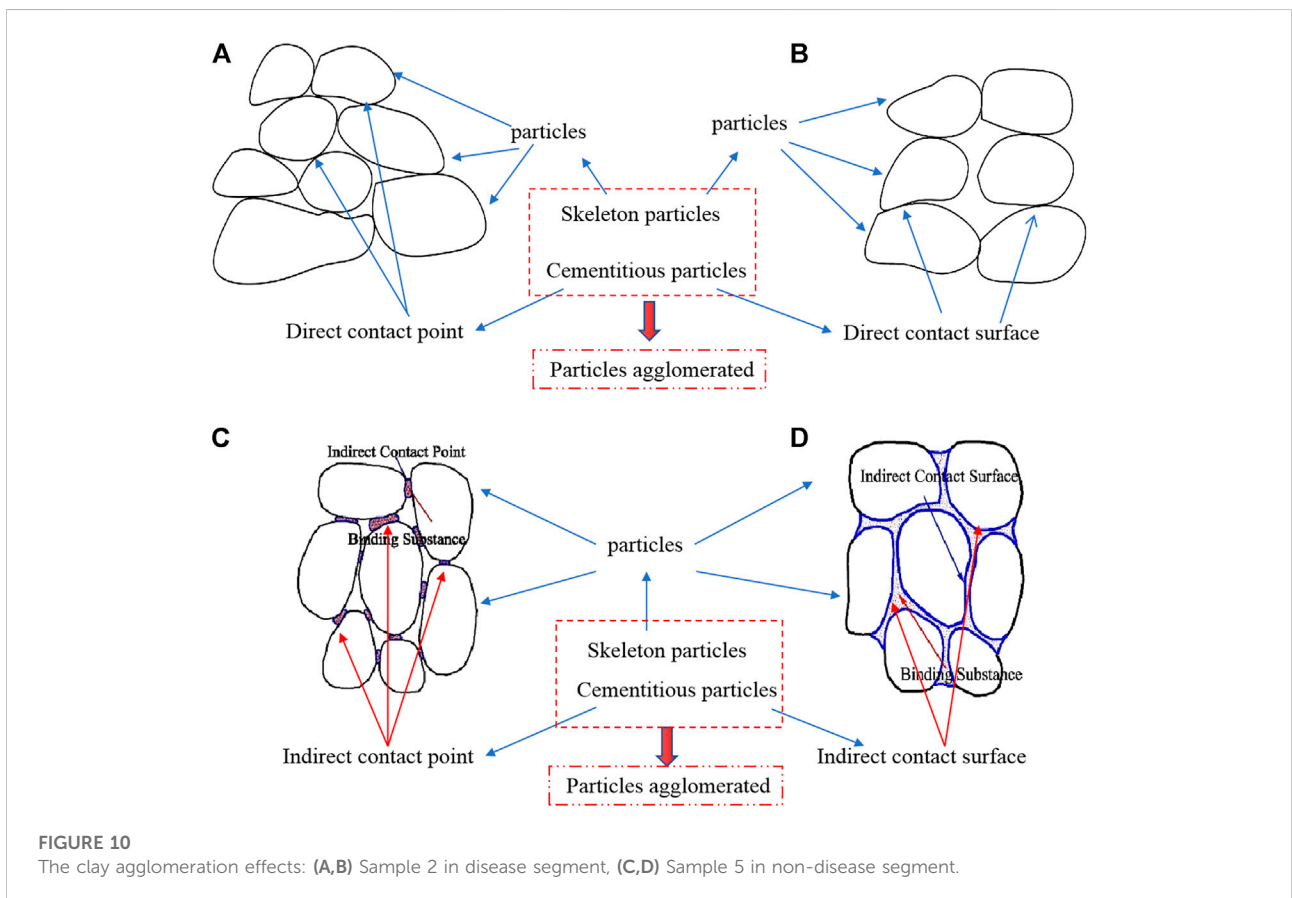


FIGURE 10
 The clay agglomeration effects: (A,B) Sample 2 in disease segment, (C,D) Sample 5 in non-disease segment.

engineering behaviors. Both particle size analysis test and XRD tests had proved that the contents of clay particles of samples in the disease segment were lower than those in non-disease segment. It was considered that the clay minerals performed a function to fill t the void in soils, and increase the internal molecular attraction. The clay fines in combination with other soil particles in loess were agglomerated. Better performances might be expected for a loess subgrade with a relatively high

content of “agglomerated” clay. In this paper, the “agglomerated” clay mineral content was defined as the difference between the clay mineral content obtained from the XRD Diffraction Test and the clay content from the particle size analysis test. The results were shown in Table 6.

Table 6 showed that the clay content of the highly compressible soil (Sample 2) in the disease segment was relatively low. Its agglomerated clay mineral content was

TABLE 6 Percentage of “agglomerated” clays in each sample.

Sample number	Clay mineral content (illite + chlorite) (%)	Clay content (%)	“Agglomerated” clay mineral content (%)
1	42	15.04	26.96
2	26	11.89	14.11
3	25	10.75	14.25
4	35	13.07	21.93
5	40	14.40	25.6
6	38	14.80	23.2

relatively low. Such level of “agglomerated” clay content could not form good attraction forces between particles. The soil (Sample 1, 4, 5, and 6) consisted of a relatively higher “agglomerated” clay mineral content and could provide relatively higher internal molecular attraction. Their structure was relatively stable when they were saturated and subjected to dynamic loads.

6 Conclusion

- 1) The results of the consolidation tests showed that in the disease segment, Samples 2 and 3, which were obtained at depths of 6 and 9 m, respectively, were highly compressible. This is considered to be a reason of the differential settlements in this area. In the non-disease segment, Samples 5 and 6, which were obtained at depths of 6 and 9 m, respectively, were relatively highly compressible. However, Sample 4, which was obtained at a depth of 3 m, has a low compressibility. Therefore, differential settlement was not observed in this area.
- 2) The results of the particle size analysis tests, XRD tests and SEM tests showed that the content of the small size particles (clay) of Samples 2 and 3 in the disease segment was relatively low, and the particle size distribution of them was poorly graded, resulting in a relatively low internal molecular attraction. It was also found that Samples 2 and 3 in the disease segment contained more than 50% of quartz and only approximately 25% of cohesive particles. The quartz content of Samples in the non-disease segment was low (<46%), but chlorite and illite-based clay mineral contents were relatively high (between 35 and 42%). In addition, the results of scanning electron microscopy test illustrated that the pores of Sample 2 in the disease segment was relatively large and dispersed. The soil particles in the disease segment were disordered and the internal molecular attraction was relatively small. The pores were small and the connectivity was poor, indicating that the soil might have a relatively poor drainage.
- 3) The experiment results in this study showed that the clay content in the loess had significant effects on the

engineering performance of the subgrade. Samples in the disease segment generally had relative low clay contents. Without enough clay particles to fill the voids in silt and fine sand, the “agglomeration” level of the soil was relatively low. When such saturated subgrade undertook dynamic loads induced by train, the soil might be liquefied and its structures became instable. If the drainage of the roadbed was not well designed, severe differential settlements might occur.

Data availability statement

The raw data supporting the conclusions of this article will be made available by the authors, without undue reservation.

Author contributions

MZ is mainly responsible for the overall planning of the thesis, H-GW and WG are responsible for on-site data processing, B-RT, CH, and RD are responsible for image processing, and Professor L-YC is responsible for the final draft of the thesis.

Funding

The research reported in this manuscript is funded by the Natural Science Foundation of China (Grants No. 41272331) and China railway academy Co.,Ltd (Grant No. 2016-KJ001-Z001-03).

Conflict of interest

Author H-GW is employed by China Northwest Research Institute Co., Ltd.

The authors declare that the research was conducted in the absence of any business or financial relationships that could be construed as potential conflicts of interest.

Publisher's note

All claims expressed in this article are solely those of the authors and do not necessarily represent those of their affiliated

organizations, or those of the publisher, the editors and the reviewers. Any product that may be evaluated in this article, or claim that may be made by its manufacturer, is not guaranteed or endorsed by the publisher.

References

- Delage, P., Cui, Y.-J., and Antoine, P. (2005). "Geotechnical problems related with loess deposits in northern France," in Proceedings of international conference on problematic soils.
- Derbyshire, E. (2001). Geological hazards in loess terrain, with particular reference to the loess regions of China. *Earth. Sci. Rev.* 54 (1), 231–260. doi:10.1016/S0012-8252(01)00050-2
- He, S., Li, P. Y., Wu, J. H., Elumalai, V., and Adimalla, N. (2020). Groundwater quality under land use/land cover changes: A temporal study from 2005 to 2015 in xi'an, northwest China. *Hum. Ecol. Risk Assess. Int. J.* 26 (10), 2771–2797. doi:10.1080/10807039.2019.1684186
- Hu, F. (2005). Treatment of foundation of wet sinking loess. *City Bridge Flood* 1, 97–98.
- Jiang, M., Zhang, F., Hu, H., Cui, Y., and Peng, J. (2014a). Structural characterization of natural loess and remolded loess under triaxial tests. *Eng. Geol.* 181, 249–260. doi:10.1016/j.enggeo.2014.07.021
- Jiang, M. J., Li, T., Hu, H. J., and Thornton, C. (2014b). DEM analyses of one-dimensional compression and collapse behaviour of unsaturated structural loess. *Comput. Geotech.* 60, 47–60. doi:10.1016/j.compgeo.2014.04.002
- Li, P., Vanapalli, S., and Li, T. (2016). Review of collapse triggering mechanism of collapsible soils due to wetting. *J. Rock Mech. Geotechnical Eng.* 8 (2), 256–274. doi:10.1016/j.jrmge.2015.12.002
- Lommler, J. C., and Bandini, P. (2015). "Characterization of collapsible soils," in IFCEE, 1834–1841.
- Luo, H., Wu, F., Chang, J., and Xu, J. (2018). Microstructural constraints on geotechnical properties of malan loess: A case study from zhaojiaan landslide in Shaanxi province, China. *Eng. Geol.* 236, 60–69. doi:10.1016/j.enggeo.2017.11.002
- Monroy, Z. L., and Ridley, A. (2010). Evolution of microstructure in compacted London clay during wetting and loading. *Géotechnique* 60 (2), 105–119. doi:10.1680/geot.8.P.125
- Muñoz-Castelblanco, J. A., Pereira, J. M., Delage, P., and Cui, Y. J. (2012). The water retention properties of a natural unsaturated loess from northern France. *Géotechnique* 62 (2), 95–106. doi:10.1680/geot.9.P.084
- Romero, E., and Simms, P. H. (2008). Microstructure investigation in unsaturated soils: A review with special attention to contribution of mercury intrusion porosimetry and environmental scanning electron microscopy. *Geotech. Geol. Eng. (Dordr.)* 26 (6), 705–727. doi:10.1007/s10706-008-9204-5
- Shao, X., Zhang, H., and Tan, Y. (2018). Collapse behavior and microstructural alteration of remolded loess under graded wetting tests. *Eng. Geol.* 233, 11–22. doi:10.1016/j.enggeo.2017.11.025
- Sun, P., Peng, J.-B., Chen, L.-W., Yin, Y.-P., and Wu, S.-R. (2009). Weak tensile characteristics of loess in China — An important reason for ground fissures. *Eng. Geol.* 108 (1), 153–159. doi:10.1016/j.enggeo.2009.05.014
- Sun, P. (2010). Reply to the discussion by ling xu on "weak tensile characteristics of loess in China — An important reason for ground fissure" by ping Sun, jian-bing peng, li-wei chen, yue-ping yin and shu-ren wu, [engineering geology 108 (2009) 153–159]. *Eng. Geol.* 114 (1), 107. doi:10.1016/j.enggeo.2010.04.008
- Susan, D. (2017). *A microstructural model for collapsing soils*. United Kingdom: Nottingham Trent University.
- Wen, B.-P., and Yan, Y.-J. (2014). Influence of structure on shear characteristics of the unsaturated loess in Lanzhou, China. *Eng. Geol.* 168, 46–58. doi:10.1016/j.enggeo.2013.10.023
- Xie, W.-L., Li, P., Zhang, M.-S., Cheng, T.-E., and Wang, Y. (2018). Collapse behavior and microstructural evolution of loess soils from the loess plateau of China. *J. Mt. Sci.* 15 (8), 1642–1657. doi:10.1007/s11629-018-5006-2
- Yan, Y., Ma, L., and Sun, Y. B. (2017). Tectonic and climatic controls on provenance changes of fine-grained dust on the Chinese Loess Plateau since the late Oligocene. *Geochimica Cosmochimica Acta* 200 (1), 110–122. doi:10.1016/j.gca.2016.12.009
- Yao, R. W., Yan, Y. T., Wei, C. L., Luo, M., Xiao, Y., and Zhang, Y. H. (2022). Hydrochemical characteristics and groundwater quality assessment using an integrated approach of the PCA, SOM and fuzzy c-means clustering: A case study in the northern sichuan basin. *Front. Environ. Sci.* 10. doi:10.3389/fev.2022.907872
- Ye, W., Yang, G., Peng, J., Huang, Q., and Xu, Y. (2012). Test research on mechanism of freezing and thawing cycle resulting in loess slope spalling hazards in Luochuan. *Yanshilixue Yu Gongcheng Xuebao/Chinese J. Rock Mech. Eng.* 31 (1), 199–205.
- Yuan, J. X. (2009). The analysis of triggering factors of loess collapsibility. *J. West-China Explor. Eng.* 31, 31–34.
- Zhang, Y. H., Dai, Y. S., Wang, Ying, Huang, X., Xiao, Y., and Pei, Q. M. (2021a). Hydrochemistry, quality and potential health risk appraisal of nitrate enriched groundwater in the Nanchong area, southwestern China. *Sci. Total Environ.* 784, 147186. doi:10.1016/j.scitotenv.2021.147186
- Zhang, Y. H., He, Z. H., Tian, H. H., Huang, X., Zhang, Z. X., Liu, Y., et al. (2021b). Hydrochemistry appraisal, quality assessment and health risk evaluation of shallow groundwater in the Mianyang area of Sichuan Basin, southwestern China. *Environ. Earth Sci.* 80 (17), 576. doi:10.1007/s12665-021-09894-y
- Zhang, Y. H., Yao, R. W., Wang, Y., Duo, J., and Cao, H. W. (2022). Zircon U–Pb and sericite Ar–Ar geochronology, geochemistry and S–Pb–Hf isotopes of the Zebuxia Pb–Zn deposit, Tibet, southwestern China. *Ore Geol. Rev.* 148, 104999. doi:10.1016/j.oregeorev.2022.104999
- Zhang, Y., Hu, Z., Li, L., and Xue, Z. (2018). Improving the structure and mechanical properties of loess by acid solutions – An experimental study. *Eng. Geol.* 244, 132–145. doi:10.1016/j.enggeo.2018.07.023
- Zhao, M., Chen, L. Y., Wang, S. Y., and Honggang, W. (2020). Experimental study of the microstructure of loess on its macroscopic geotechnical properties of the Baozhong railway subgrade in Ningxia, China. *Bull. Eng. Geol. Environ.* 79 (9), 4829–4840. doi:10.1007/s10064-020-01816-9
- Zhao, M., Guo, W., Chen, L. Y., and Wang, S. Y. (2019). Experiment on the frost resistance of modified phospho gypsum: A case used to improve Baozhong railway subgrade loess. *J. Mt. Sci.* 16 (12), 2920–2930. doi:10.1007/s11629-018-5014-2
- Zhao, S., and Lei, Y. (2011). "The autonomous robot object recognition algorithm based on multi-feature fusion," in Paper presented at the 2011 international conference on electric information and control engineering. doi:10.1109/ICEICE.2011.5777691
- Zhuang, J., Peng, J., Wang, G., Javed, I., Wang, Y., and Li, W. (2018). Distribution and characteristics of landslide in Loess Plateau: A case study in Shaanxi province. *Eng. Geol.* 236, 89–96. doi:10.1016/j.enggeo.2017.03.001